Preparation and Characterization of Carbon Nanotubes−Polymer/Ag Hybrid Nanocomposites via Surface RAFT Polymerization

Xiaowei Pei,[†,‡] Jingcheng Hao,[†,§,*] and Weimin Liu[†,*]

State Key Laboratory of Solid Lubrication, Lanzhou Institute of Chemical Physics, Chinese Academy of Sciences, Lanzhou 730000, P. R. China, Graduate School of Chinese Academy of Sciences, Beijing 100039, P. R. China, and Key Laboratory of Colloid and Interface Chemistry (Shandong University), Ministry of Education, Jinan 250100, P. R. China

Polymer brushes with multiwalled carbon nanotubes (MWNTs) as backbones were synthesized by grafting 2-hydroxyethyl methacrylate (HEMA) from the sidewall of MWNTs via surface reversible addition and fragmentation chain transfer (RAFT) polymerization using RAFT agent immobilized MWNTs as chain transfer agent. After immobilization of the RAFT agent, poly(2-hydroxyethyl methacrylate) (PHEMA) chains as water-soluble polymer chains were successfully grafted from the surface of MWNTs, resulting in the formation of core−shell nanostructures. Fourier transform infrared spectroscopy, thermal gravimetric analysis, and X-ray photoelectron spectroscopy were used to determine chemical structure and the grafted polymer quantities of the resulting product. Transmission electron microscopy (TEM) images indicated that the nanotubes were coated with a polymer layer. Gel permeation chromatography analyses showed that the molecular weight of cleaved PHEMA increased linearly with the grafted polymer content and the cleaved PHEMA chains had a narrow molecular weight distribution. The PHEMA grafted MWNTs can be hydrolyzed by HCl solution to yield poly(methacrylic acid) (PMAA) grafted MWNTs, which have higher loading capacities for metal ions, such as Ag^+. TEM and energy dispersive spectroscopy measurements confirmed the nanostructures and the components of the resulting MWNT-PMAA/Ag hybrid nanocomposites.

Introduction

Carbon nanotubes (CNTs) have attracted worldwide attention since their discovery by Iijima in 1991[1] due to possessing unique properties in the fields of nanoscience, nanotechnology, and bioengineering. Functionalization of carbon nanotubes is expected to play a vital role in tailoring the structure and properties of CNTs, improving the solubility and compatibility of CNTs, and preparing novel CNT-based nanodevices, nanocomposites.[2] However, since carbon nanotubes are large molecules with thousands of carbon atoms in an aromatic delocalized system, they are practically insoluble in all solvents and are, consequently, difficult to handle.[3] Therefore, many research groups have focused on functionalizing CNTs with various organic and organometallic structures and linear polymers to increase their solubility.[4]

Grafting polymer onto the surface of carbon nanotubes has recently attracted considerable attention because it endows the surface with novel structures and properties. So-called "grafting to" and "grafting from" approaches have been employed to attach polymer chains onto the surface of CNTs. The "grafting to" route involves the bonding of a performed end-functionalized polymer chains to the reactive surface of the CNTs by amidation, esterification, radical coupling, or other reactions.[5] Generally, the grafted polymer content is quite limited due to the relatively low reactivity of polymer.[6] In contrast, the "grafting from"

technique, which generally involves the immobilizing of initiators onto the CNTs surface followed by in situ surface-initiated polymerization to generate the tethered polymer chains.[7−12] The advantage of this technique is that many kinds of polymer chains with high grafting density are easily attached on the surface of CNTs.

Recently, many "living/controlled" polymerization techniques were applied to surface-initiating graft polymerization. Successful examples of the "living/controlled" polymerization include atom transfer radical polymerization (ATRP)[13,14] and reversible addition−fragmentation chain transfer (RAFT) polymerization.[15−17] Because of the capability to control the polymerization of a wide variety of monomers without using metal catalysts and the mild reaction conditions, RAFT polymerization has received increasing attention. However, compared with the large number of reports using ATRP to prepare polymer grafted substrates, there are surprisingly few reports on the application of RAFT techniques to the synthesis of polymer grafted substrates, probably due to the difficulty to covalently attach RAFT agent to a substrate.

Herein, a versatile route is reported for preparing RAFT agent anchored multiwalled carbon nanotubes and then grafting the poly(2-hydroxyethyl methacrylate) (PHEMA) chains from the surface of carbon nanotubes via RAFT polymerization. Furthermore, to explore potential applications of these PHEMA grafted carbon nanotubes, we further derivatized the 2-hydroxylethyl ester groups into carboxylic acids. Then the resulting poly(methacrylic acid)-coated carbon nanotubes were used to sequester Ag^+ and hence to prepare CNTs−polymer/Ag hybrid nanocomposites. Scheme 1 presents the overall synthesis route.

* Corresponding authors. E-mail: (J.H.) jhao@sdu.edu.cn; (W.L.) wmliu@lzb.ac.cn. Fax: +86-931-8277088.
† Lanzhou Institute of Chemical Physics, Chinese Academy of Sciences.
‡ Graduate School of Chinese Academy of Sciences.
§ Shandong University.

SCHEME 1: Outlines of the Surface RAFT Polymerization of HEMA from MWNT and Metal Loading

SCHEME 2: Synthesis of RAFT Agent 4-(4-Cyanopentanoic Acid) Dithiobezoate (CPAD)
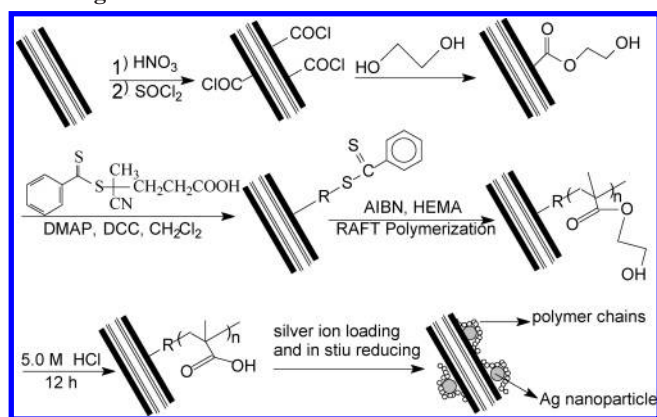
Experimental Section

Materials. The multiwalled carbon nanotubes (MWNTs) (Shenzhen Nanotech Port Co., Ltd., China) were made from the chemical vapor deposition method ($>95\%$ purity, $<3\%$ amorphous, $<2\%$ ash, special surface area $450-600$ m^2/g). 4,4′-Azobis-(4-cyanopentanoic acid) (ACPA) (Fluka, $>98\%$) and 2-hydroxyethyl methacrylate (HEMA, Acros, $>98\%$) were purified by vacuum distillation, azobisisobutylnitrile (AIBN) (AR, Shanghai First Chemical Reagent Factory) was purified by recrystallization from ethanol, and tetrahydrofuran (THF) was refluxed over sodium and distilled twice before use. Dithiobenzoic acid (DTBA) was prepared according to a reported method[18] in 65% yield. ^{1}H NMR (400 MHz, δ, ppm, CDCl$_3$): 8.02 (d, 2H, *o*-Ar*H*), 7.60 (t, 1H, *p*-Ar*H*), 7.40 (*t*, 2H, m-Ar*H*). Dichloromethane (DCM) was dried over CaH$_2$ and distilled prior to use. Glycol (HOCH$_2$CH$_2$OH, $\geq99\%$) and AgNO$_3$ (99.9999%) were used directly, and all other regents were used without further purification.

Characterization and Instrumentation. X-ray photoelectron spectra (XPS) were performed on a PHI-5702 instrument using Mg Kα radiation with a pass energy of 29.35 eV. Gel permeation chromatography (GPC) analysis of the samples were carried out on an HP 1100 HPLC, *N,N*-dimethylformamide (DMF) was used as the mobile phase, and monodispersed polystyrene standards were used to generate the calibration curve. Hydrogen nuclear magnetic resonance (^{1}H NMR) spectra were measured with an INOVA 400 MHz spectrometer. Fourier transform infrared (FTIR) spectra were recorded on an IFS 66v/S FTIR spectrometer (Bruker, Germany) using the KBr disk method. Thermal gravimetric analyses (TGA) were carried out on a Perkin-Elmer TGA-7 instrument with a heating rate of 10 °C/min under nitrogen. Transmission electron microscopy (TEM) analyses were conducted on a Hitachi Model H-600 electron microscope at 100 kV. Scanning electron microscopy (SEM) images and relevant elements analysis were examined using a JEM-1200EX (JEOL, Japan) microscope equipped with a Kevex energy dispersive spectrometer (EDS) analyzer, and the samples were loaded on the copper substrate, previously sputter-coated with a homogeneous gold layer for charge dissipation during the SEM imaging.

Acid Treatment of MWNTs. A 100 mL flask charged with 2.0 g of crude MWNTs and 30 mL of 60% HNO$_3$ aqueous solution was sonicated in a bath (40 kHz) for 30 min and stirred for 20 h at reflux. After cooling to room temperature, the mixture was vacuum-filtered through a 0.22 μm polycarbonate membrane and washed with distilled water until the pH of the filtrate
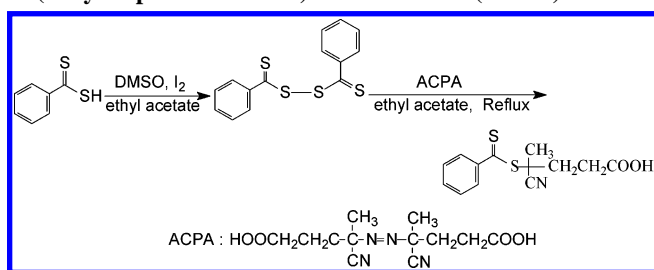
was 7.0. The filtered solid was dried under vacuum for 24 h at 60 °C to give about 1.3 g of carboxylic acid-functionalized MWNT (MWNT-COOH).[19]

Synthesis of MWNT-OH. Dried MWNT-COOH (1.0 g) was reacted with excess neat SOCl$_2$ (25 mL) at 70 °C for 24 h. The residual SOCl$_2$ was removed under vacuum. The remaining solid (MWNT-COCl) was immediately reacted without further purification with glycol (40 mL) for 48 h at 120 °C. Then the solid was separated by vacuum filtration using a 0.22 μm polycarbonate membrane and washed with anhydrous THF. After repeated washing and filtration, the resulting solid was dried overnight in a vacuum to give 0.82 g of hydroxyl group-functionalized MWNT (MWNT-OH).

Synthesis of RAFT Agent 4-(4-Cyanopentanoic Acid) Dithiobezoate (CPAD). The target compound was prepared according to a modification method of Thang et al.[20] Typically, the DTBA (60 mmol) and a catalytic amount of I$_2$ (0.1 g) were dissolved in 30 mL of ethyl acetate in a 100 mL flask. Into this solution, a solution of dimethyl sulfonyl oxide (DMSO) (30 mmol) in 10 mL of ethyl acetate was added slowly while stirring vigorously. The reaction mixture was stirred in the dark for 10 h. Without further purification, the crude disulfide was used directly in the next step. 4,4′-Azobis-(4-cyanopentanoic acid) (46 mmol) and 30 mL of ethyl acetate were added into the flask. The mixture was stirred at reflux for 18 h. The ethyl acetate was removed under reduced pressure. The crude product was isolated by silica gel column chromatography using ethyl acetate:hexane (1:2) as eluent. Those fractions in pink red were combined. The solvent was removed in vacuo to give a red solid. ^{1}H NMR (400 MHz, δ, ppm, CDCl$_3$): 1.95 (s, 3H, $-$CH$_3$), $\sim$2.40$-$2.80 (m, 4H, $-$CH$_2$CH$_2-$), 7.40 (t, 2H, *m*-ArH), 7.59 (t, 1H, *p*-ArH), 7.91 (d, 2H, *o*-ArH) (see Scheme 2).

Immobilization of the RAFT Agent on the MWNT Surface. The compound CPAD (2.80 g, 10 mmol) and MWNT-OH (0.60 g) were dissolved in 25 mL of anhydrous DCM. After dicyclohexylcarbodiimide (DCC) (2.27 g, 11 mmol) and (dimethylamino) pyridine (DMAP) (0.12 g, 1 mmol) were added to the solution, the mixture was stirred at room temperature in the dark for 24 h. After the reaction, the solid was filtered and washed five times with 100 mL of CH$_2$Cl$_2$. Then the raw product was dispersed in 200 mL of distilled water and recovered by centrifugation. At last, the solid was re-dispersed in 100 mL of THF, sonicated for 15 min, separated by vacuum filtration using a 0.22 μm polycarbonate membrane, and washed with anhydrous THF four times. Then the resulting solid was dried overnight under vacuum at room temperature to give 0.51 g of RAFT agent immobilized MWNT (MWNT-SC(S)Ph). TGA showed 17.7% weight loss below 500 °C for MWNT-SC(S)Ph and 10.9% weight loss for MWNT-OH. This 6.8% difference in weight loss corresponds to $\sim$0.244 mmol RAFT agent groups per gram of MWNT-SC(S)Ph.

Synthesis of MWNT-PHEMA by Surface RAFT Method. MWNT-SC(S)Ph (40.0 mg, 9.76 μmol), HEMA(0.63 g, 4.85

Carbon Nanotubes−Polymer/Ag Hybrid Nanocomposites

J. Phys. Chem. C, Vol. 111, No. 7, 2007 **2949**

mmol), and *N,N*-dimethylformamide (DMF) (2 mL) were added into a 10 mL dry flask, which was then sealed with a rubber plug. After sonication for 5 min, the flask was evacuated and filled with nitrogen three times. AIBN (49.0 μL of 0.050 M DMF solution) was injected into the flask using a syringe. The flask was immersed in an oil bath at 70 °C immediately and kept stirring for some times. By the end of the reaction the viscosity had increased dramatically. The polymerization was stopped by quenching the flask in ice water, and the polymerization mixture was diluted with 200 mL of DMF, bathsonicated for 30 min, and filtered through a 0.22 μm polycarbonate membrane. To ensure that no ungrafted polymer or free reagents were mixed in the product, the filtered solid was redispersed in methanol, then filtered, and washed with methanol five times. A gray solid powder was obtained after vacuumdrying for 24 h.

Cleavage of PHEMA from MWNT. PHEMA chain can be cleaved from the MWNT at ester bond under basic conditions. Typically, the MWNT-PHEMA (50 mg) was dispersed in 40 mL of 1 M NaOH/ethanol (1:2) solution and stirred under reflux for 72 h, then filtered though a 0.22 μm polycarbonate membrane, resulting in the defunctionalized MWNT and detached PHEMA. The filtrate was filtered and evaporated to dryness. The remaining polymer was redissolved in methanol and filtered. Then the homoPHEMA was obtained by removal of methanol and dried in a vacuum. The molecular weight of homoPHEMA was analyzed by GPC.

Hydrolysis of MWNT-PHEMA To Synthesize Poly-(methacrylic acid)-Coated MWNT. The ester groups of PHEMA can be partially hydrolyzed into carboxyl groups by the following procedure: After MWNT-PHEMA (60 mg) was dispersed in 2 mL of DMF, 8 mL of 5 M hydrochloride acid was added, and the mixture was heated to reflux and kept at this temperature for 12 h. The reaction mixture was separated by centrifugation. The collected solid was washed with excess water and then alcohol. A dust-color solid powder was obtained after vacuum-drying for 24 h.

Preparation of MWNT-PHEMA/Ag Hybrid Nanocomposites. The plentiful carboxyl groups in poly(methacrylic acid) (PMAA) can be used to chelate Ag^+, giving rise to MWNT-PMAA/Ag hybrid nanocomposites. Typically, a 100 mL flask charged with 50 mg of MWNT-PMAA and 20 mL of distilled water was sonicated in a bath (40 kHz) for 10 min, and the $AgNO_3$ aqueous solution (20 mL, 0.01 M) was added dropwise with vigorous stirring. The mixture was stirred at room temperature in the dark for 12 h and separated by centrifugation. The collected solid was dispersed in distilled water (40 mL), and $NaBH_4$ solution (8 mL, 0.1 M) was added dropwise with vigorous stirring for 2 h in 40 °C and separated by centrifugation. The collected solid was re-dispersed in distilled water (20 mL) and recovered by centrifugation again. A gray solid powder was obtained after vacuum-drying for 24 h.

Results and Discussion

Immobilization of RAFT Agent onto MWNTs Surfaces. It is well-known that dithiobenzoate is an excellent RAFT agent for living radical polymerization of (meth)acrylate and styrene monomers, so we should immobilize dithiobenzoate onto MWNTs surface in order to prepare polymer grafted MWNTs. After treatment with nitric acid, MWNTs were functionalized with carboxylic groups, and the carboxylic groups functionalized MWNTs were treated with thionyl chloride, then reacted without further purification with glycol to give hydroxyl group-functionalized MWNTs (MWNT-OH). The RAFT agent immobi-
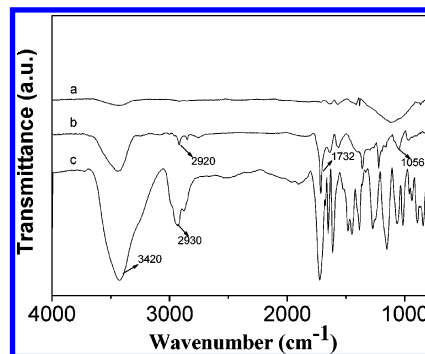

Figure 1. FTIR spectra of (a) crude MWNT, (b) MWNT-SC(S)Ph, (c) MWNT-PHEMA.
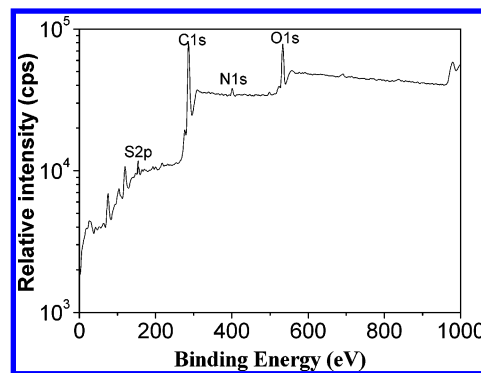

Figure 2. XPS full-scan spectrum of the MWNT-SC(S)Ph.

lized MWNTs (MWNT-SC(S)Ph) were prepared by the reaction of MWNT-OH with RAFT agent 4-(4-cyanopentanoic acid) dithiobezoate (CPAD) in the presence of DCC and DMAP. The MWNT-SC(S)Ph was then characterized by FTIR measurements. The amount of sample added to the KBr must be strictly controlled because the black MWNTs can absorb the infrared rays if the MWNTs added were too much. Compared with crude MWNTs (Figure 1a), the FTIR spectra of MWNT-SC(S)Ph (Figure 1b) clearly shows the characteristic peaks of RAFT agent such as C−H, C=O, and C=S stretching vibrations centered at 2920, 1732, and 1056 cm^{-1}, respectively. X-ray photoelectron spectroscopy (XPS) analysis can be employed to determine the composition of the RAFT agent immobilized MWNTs. Figure 2 shows the XPS full-scan spectrum of the MWNT-SC(S)Ph. The peaks at the binding energies of about 284.6, 533.2, 399.5, and 162.5 eV are attributed to the C1s, O1s, N1s, and S2p, respectively. Judging by combination of FTIR and XPS results, we can conclude that the RAFT agent has covalently bound to the surface of MWNTs.

Preparation of MWNT-PHEMA via Surface RAFT Polymerization. The preparation of MWNT-PHEMA was illustrated in Scheme 1. HEMA was polymerized using AIBN as initiator and MWNT-SC(S)Ph as chain transfer agent. After some time of polymerization at 70 °C, the viscosity of the reaction system had increased dramatically, indicating that the surface RAFT polymerization had taken place. Then through filtrating, washing, and drying the product, gray powder was obtained. The color of product turned from black to gray with increasing polymer content. Table 1 summarizes the reaction conditions and results.

The PHEMA chains of MWNT-PHEMA were cleaved from MWNTs at ester bond under basic condition. Then the molecular weight (MW) and the molecular weight distribution of obtained homoPHEMA were analyzed by GPC. The grafted polymer content (f_{wt} %, calculated from TGA data) vs polymerization time was plotted as shown in Figure 3. The grafted polymer

TABLE 1: Polymerization Conditions and Some Results

| sample	R^a	time (h)	f_{wt} (%)[b]	$M_{n,GPC}$	M_w/M_n
homo-PHEMA	$2500:10:1^c$	10	100	14200	1.18
MPH1	2000:4:1	8	26.3	5700	1.53
MPH2	2000:4:1	16	42.3	8900	1.42
MPH3	2000:4:1	24	69.2	13100	1.40
MPH4	2000:4:1	32	78.4	15200	1.35

[a] $R =$ monomer:MWNT-SC(S)Ph:AIBN (mol:mol:mol). [b] $f_{wt} =$ the polymer content of the product calculated from TGA data. [c] Monomer: RAFT agent:AIBN $= 2500:10:1$ (mol:mol:mol).
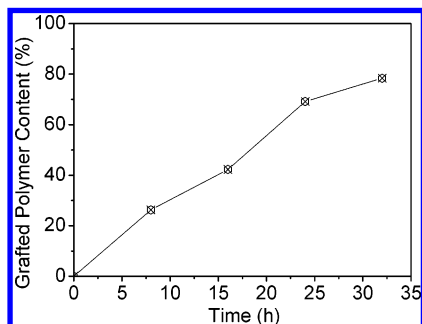
Figure 3. Relationships of the grafted polymer content with polymerization time.
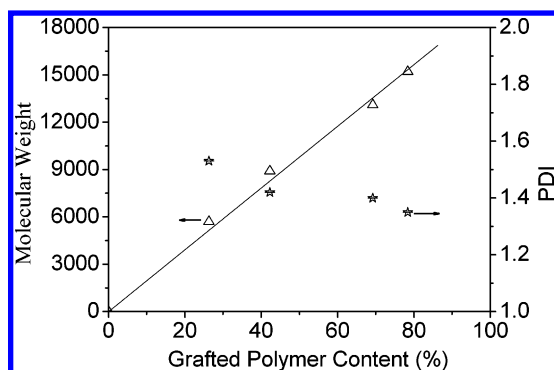
Figure 4. Variations of molecular weight and PDI of cleaved PHEMA with grafted polymer content.

content (f_{wt} %) exhibited a nearly linear increase of polymerization time. The molecular weight of cleaved PHEMA increased linearly with the grafted polymer content (f_{wt} %) as shown in Figure 4, indicating that the length of PHEMA chains on MWNTs is controllable. Moreover, GPC analyses of the cleaved PHEMA showed that the PHEMA chains on MWNT had a narrow molecular weight distribution. Therefore, the above results revealed that this RAFT polymerization of HEMA from MWNTs surface is controlled.

Characterization of MWNT-PHEMA. The FTIR spectrum of MWNT-PHEMA is shown in Figure 1c. After polymerization, a strong peak around 3400 cm^{-1} due to O−H stretching and an increase in the intensity around 2930 cm^{-1} due to C−H stretching were observed which correlated with the structure of PHEMA, and the characteristic adsorption peaks assigned to carbonyl (C=O) vibrations were clearly visible at 1732 cm^{-1}. These results indicated that polyHEMA chains had successfully grafted from the surface of MWNTs via RAFT polymerization.

Figure 5 displays the TGA weight loss curves of some samples of pristine MWNTs, MWNT-OH, MWNT-SC(S)Ph, MWNT-PHEMA, and homo-PHEMA. The weight loss of pristine MWNTs below 450 °C is less than 3%. There is an
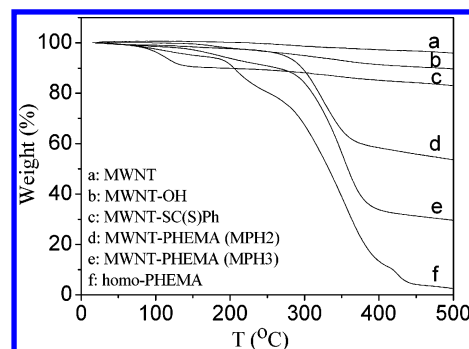
Figure 5. TGA curves of (a) crude MWNT, (b) MWNT-OH, (c) MWNT-SC(S)Ph, (d, e) MWNT-PHEMA, and (f) homoPHEMA.
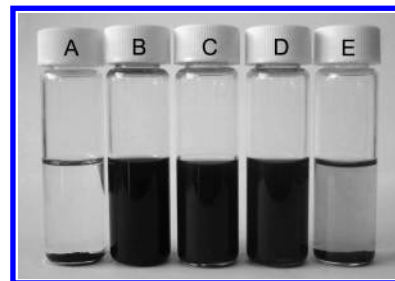
Figure 6. Photo of MWNT-SC(S)Ph in water (A), MWNT-PHEMA in methanol (B) and water (C), MWNT-PMAA in water (D), and MWNT-SC(S)Ph (20%) and homoPHEMA (80%) into water (E).
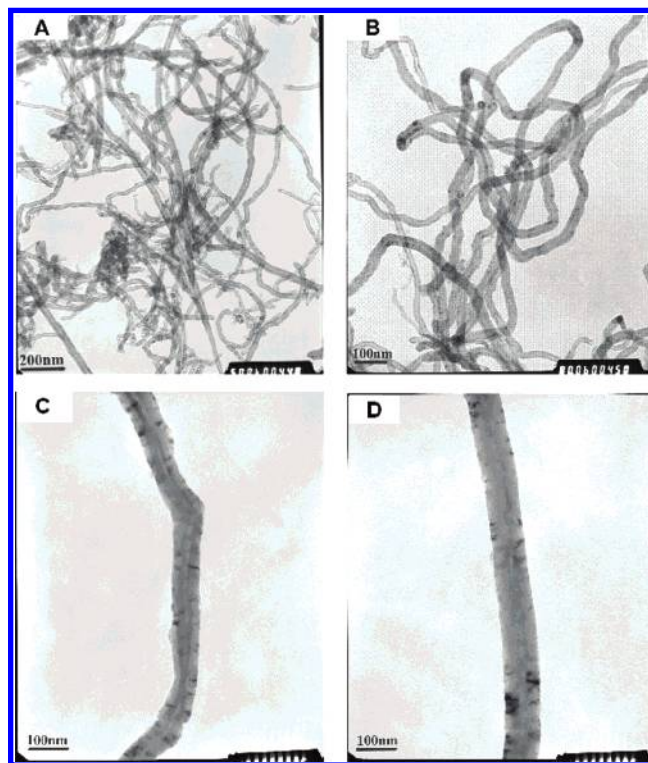
Figure 7. TEM image of the crude MWNT (A), MWNT-SC(S)Ph (B), MPH2 (C), and MPH4 (D).

obvious weight loss stage between 100 and 450 °C for MWNT-OH (10.9%) and MWNT-SC(S)Ph (17.7%). A 6.8% difference in weight loss corresponds to ~0.244 mmol RAFT agent groups per gram of MWNT-SC(S)Ph. Compared with pristine MWNTs, TGA of MWNT-PHEMA showed one major decomposition at a temperature range from 280 to 420 °C corresponding to surface grown PHEMA on MWNTs. The content of the polymer shell calculated from the TGA data varies from 26.3% to 78.4% when
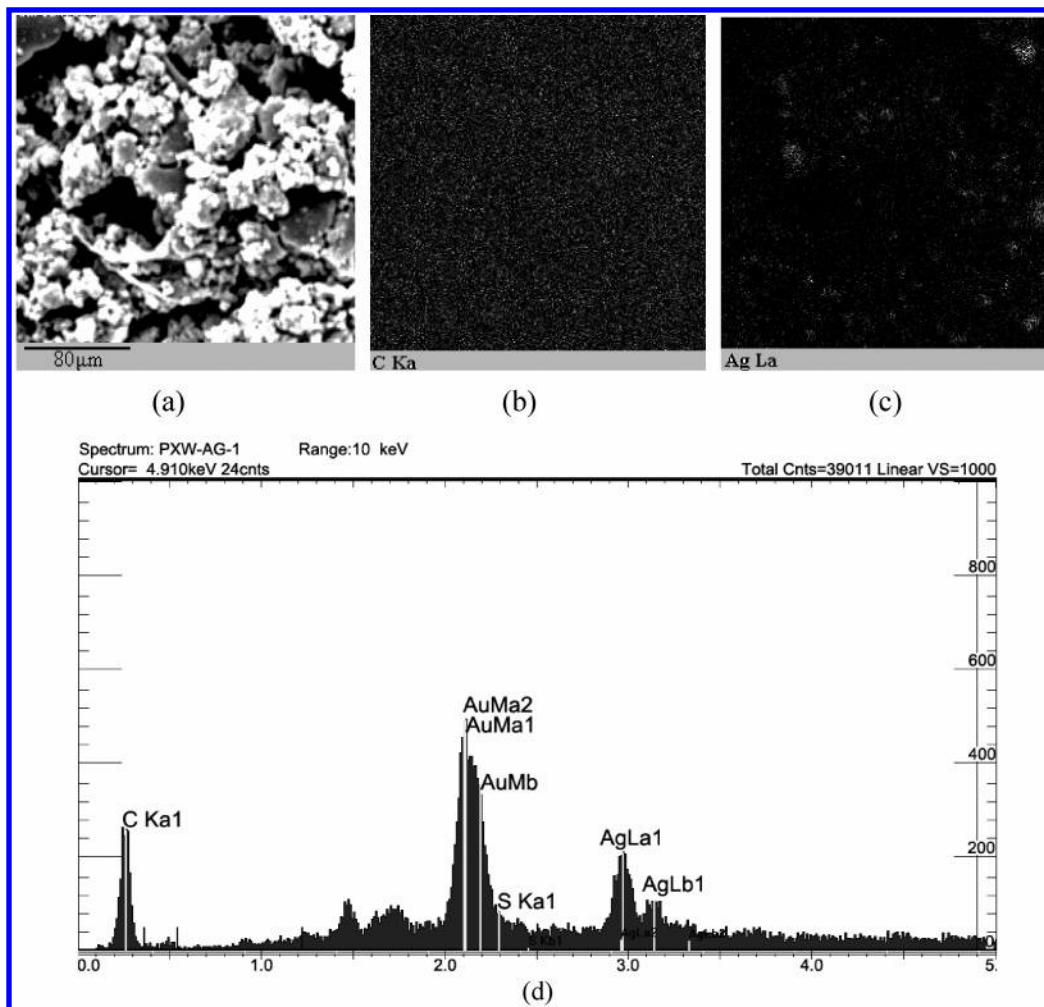
Figure 8. Scanning electron microscopy (SEM) and energy dispersive spectroscopy (EDS) analysis of MWNT-PMAA/Ag hybrid nanocomposites: (a) SEM image of EDS analysis area, (b) carbon elemental mapping, (c) silver elemental mapping, and (d) EDS spectrum.
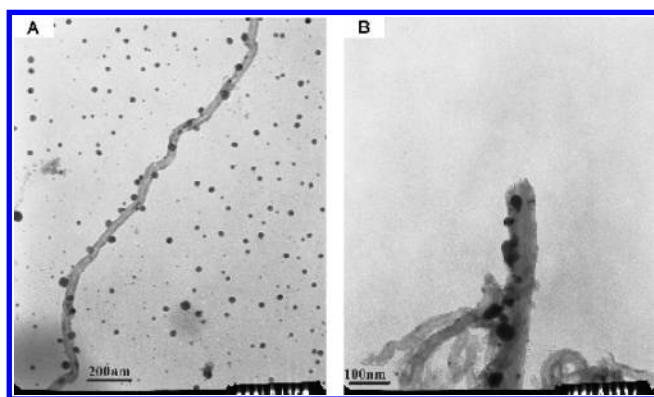

Figure 9. TEM image of MWNT-PMAA/Ag hybrid nanocomposites (A, B).

polymerization time increased from 8 to 32 h, which can be seen from Table 1.

Dispersion of MWNT-SC(S)Ph into aqueous solution or organic solvent was very difficult even after it was sonicated; sedimentation of MWNT-SC(S)Ph appeared a few minutes after sonication. However, dispersion of MWNT-PHEMA into aqueous solution or organic solvent was very easy. So the solubility or dispersibility of the functionalized MWNTs strongly depends on the structure and amounts of the grafted organic moieties. Figure 6 gives the digital photos of the MWNT-SC(S)Ph in distilled water and MWNT-PHEMA in methanol and distilled water. It is clear that MWNT-SC(S)Ph is insoluble in distilled

water, and there was much sedimentation of MWNT-SC(S)Ph at the bottom of the vial. However, the MWNT-PHEMA is soluble in methanol and distilled water, forming a homogeneous solution, and there was no sedimentation observed even after ten days as shown in Figure 6B,C. After hydrolysis of MWNT-PHEMA, the resulting product MWNT-PMAA showed a very good solubility in distilled water, but it is not soluble in weakly polar and nonpolar solvents such as THF, CHCl$_3$, and toluene. As shown in Figure 6D, the aqueous solution of MWNT-PMAA keeps stable for more than 1 month. For comparison, we attempted to disperse the mixture MWNT-SC(S)Ph (20%) and homoPHEMA (80%) into distilled water, but it is shown that homoPHEMA is a poor dispersant for MWNTs in distilled water. All of the evidence indicates that the solubilization of the MWNTs was by covalently bound PHEMA chains on the surface of MWNTs and not adsorbed homoPHEMA.

The morphological structures of pristine, RAFT agent immobilized, and PHEMA grafted MWNTs were examined by TEM. Figure 7 shows TEM images of the crude MWNTs, MWNT-SC(S)Ph, and MWNT-PHEMA. The average diameters of the crude nanotubes are about 30 nm. The MWNT wall consists of 10−25 graphite layers. The average length of the MWNT is approximately several micrometers. In the images of crude MWNTs (Figure 7A), it is clear that many pristine MWNTs were piled up. The crude MWNTs surface is featureless, and there are little or no traces of amorphous carbon. However, it can be found that after immobilization of RAFT

agents onto the surface of MWNTs, the dispersibility of MWNT-SC(S)Ph increased, which results from the good solubility of the MWNT-SC(S)Ph in solvent (Figure 7B).

As for MWNT-PHEMA (Figure 7C,D), it can be seen that the nanotubes are coated with a polymer layer. The polymer shell surrounding an individual nanowire is very uniform. In addition, the images also indicated that the grown polymer chains can contribute to the dispersibility of massed tubes, and the average thickness of the polymer layer increases with increasing of polymer content. These results indicated that crude MWNTs can be separated into individual tube by surface RAFT polymerization of HEMA.

Hydrolysis of MWNT-PHEMA and Metal Loading. The ester groups of PHEMA can be partially hydrolyzed into carboxyl groups by refluxing the MWNT-PHEMA in a solution of hydrochloride (5.0 M) aqueous for 12 h. Then a gray or black solid powder (MWNT-PMAA) was obtained after vacuum-drying for 24 h. The plentiful carboxyl groups in PMAA can be used to chelate Ag^+, giving rise to MWNT-PMAA/Ag hybrid nanocomposites. Compared with the use of pristine or oxidized CNTs as templates to adsorb metal ions (e.g., Ag^+, Pd^{2+}, Cu^{2+}, and Cd^{2+}),[21,22] here we using the grafted PMAA chains to sequester Ag^+ in order to prepare MWNT-PMAA/Ag hybrid nanocomposites. Polymer grafted MWNTs as templates to chelate metal ions have some advantages,[23] such as (1) the metal ion loading can be controlled by the grafted polymer density, (2) the metal-loaded MWNTs are relatively stable due to the protective nature of the polymer overlayer, and (3) hybrid polymer/metal nanocomposites can be readily obtained.

The components and their distributions of the resulting MWNT-PMAA/Ag hybrid nanocomposites were conducted using an SEM instrument equipped with an energy dispersive spectrometer (EDS) analyzer. Figure 8 shows the morphology, elemental mapping and EDS result of the MWNT-PMAA/Ag hybrid nanocomposites. As shown in Figure 8a, because of the high polymer loading, the morphology of the underlying nanotubes is rarely observed. EDS analysis confirmed a high silver concentration (Figure 8d). The carbon map is relatively symmetric and smooth, matching with the SEM morphology (Figure 8b). The map of silver indicated that the distribution of silver was relatively uniform and also matched the SEM morphology (Figure 8c).

The MWNT-PMAA/Ag hybrid nanocomposites were also examined by TEM (Figure 9). Figure 9A indicates that Ag nanoparticles loaded nanotubes can be clearly observed, and separated nanoparticles with an average diameter ca. 20 nm were also found within the composites, which suggests that the unattached nanoparticles have not been completely removed from the product. In Figure 9B, Ag nanoparticles decorated nanotube was obtained.

Conclusions

The preparation of RAFT agent immobilized MWNTs and the functionalization of MWNTs with PHEMA via surface RAFT polymerization were wholly investigated in this work. After immobilization of the RAFT agent, PHEMA chains as water-soluble polymer chains were successfully grafted from the surface of MWNTs via surface RAFT polymerization, resulting in the formation of core−shell nanostructures, with the PHEMA as the brush-like or hairy shell, and the MWNTs as the hard backbone. The covalent bonding of PHEMA to the MWNTs dramatically improved the water solubility of MWNTs. The molecular weight of cleaved PHEMA increased linearly with the grafted polymer content indicating that the length of

PHEMA chains on MWNTs is controllable. Moreover, GPC analyses showed that the cleaved PHEMA chains had a narrow molecular weight distribution. TEM observations showed that the nanotubes were coated with polymer layer. TGA results indicate that the grafted polymer content varies from 26.3% to 78.4% when polymerization time increased from 8 to 32 h. The PHEMA grafted MWNTs can be hydrolyzed by HCl solution to yield PMAA grafted MWNTs, which have higher loading capacities for metal ions, such as silver ion. TEM and EDS measurements confirmed the nanostructures and the components of the resulting MWNT-PMAA/Ag hybrid nanocomposites.

References and Notes

(1) Iijima, S. *Nature* **1991**, *354*, 56−58.

(2) (a) Liu, J.; Rinzler, A. G.; Dai, H. J.; Hafner, J. H.; Bradley, R. K.; Boul, P. J.; Lu, A.; Iverson, T.; Shelimov, K.; Huffman, C. B.; Rodriguez-Macias, F.; Shon, Y. S.; Lee, T. R.; Colbert, D. T.; Smalley, R. E. *Science* **1998**, *280*, 1253−1256. (b) Chen, J.; Hamon, M. A.; Hu, H.; Chen, Y.; Rao, A. M.; Eklund, P. C.; Haddon, R. C. *Science* **1998**, *282*, 95−98. (c) Ajayan, P. M. *Chem. Rev.* **1999**, *99*, 1787−1799. (d) Dai, H. *Acc. Chem. Res.* **2002**, *35*, 1035−1044. (e) Bianco, A.; Prato, M. *Adv. Mater.* **2003**, *15*, 1765−1768.

(3) Cui, J.; Wang, W. P.; You, Y. Z.; Liu, C. H.; Wang, P. H. *Polymer* **2004**, *45*, 8717−8721.

(4) (a) Qin, S.; Qin, D.; Ford, W. T.; Resasco, D. E.; Herrera, J. E. *Macromolecules* **2004**, *37*, 752−757. (b) Kong, H.; Li, W.; Gao, C.; Yan, D.; Jin, Y.; Walton, D. R. M.; Kroto, H. W. *Macromolecules* **2004**, *37*, 6683−6686. (c) Hong, C.-Y.; You, Y.-Z.; Wu, D.; Liu, Y.; Pan, C.-Y. *Macromolecules* **2005**, *38*, 2606−2611. (d) Chen, S.; Wu, G.; Liu, Y.; Long, D. *Macromolecules* **2006**, *39*, 330−334. (e) Qin, S.; Qin, D.; Ford, W. T.; Resasco, D. E.; Herrera, J. E. *J. Am. Chem. Soc.* **2004**, *126*, 170−176. (f) Liu, P. *Eur. Polym. J.* **2005**, *41*, 2693−2703.

(5) Mansky, P.; Liu, Y.; Huang, E.; Russell, T. P.; Hawker, C. J. *Science* **1997**, *275*, 1458−1460.

(6) Cao, L.; Yang, W.; Yang, J.; Wang, C.; Fu, S. *Chem. Lett.* **2004**, *33*, 490−491.

(7) Matyjaszewski, K.; Miller, P. J.; Shukla, N.; Immaraporn, B.; Gelman, A.; Luokala, B. B.; Siclovan, T. M.; Kickelbick, G.; Vallant, T.; Hoffmann, H.; Pakula, T. *Macromolecules* **1999**, *32*, 8716−8724.

(8) Husseman, M.; Malmström, E. E.; McNamara, M.; Mate, M.; Mecerreyes, D.; Benoit, D. G.; Hedrick, J. L.; Mansky, P.; Huang, E.; Russell, T. P.; Hawker, C. J. *Macromolecules* **1999**, *32*, 1424−1431.

(9) Vestal, C. R.; Zhang, Z.-J. *J. Am. Chem. Soc.* **2002**, *124*, 14312−14313.

(10) Jordan, R.; Ulman, A. *J. Am. Chem. Soc.* **1998**, *120*, 243−247.

(11) Jordan, R.; Ulman, A.; Kang, J. F.; Rafailovich, M. H.; Sokolov, J. *J. Am. Chem. Soc.* **1999**, *121*, 1016−1022.

(12) Weck, M.; Jackiw, J. J.; Rossi, R. R.; Weiss, P. S.; Grubbs, R. H. *J. Am. Chem. Soc.* **1999**, *121*, 4088−4089.

(13) Zhao, H.; Farrell, B. P.; Shipp, D. A. *Polymer* **2004**, *45*, 4473−4481.

(14) Kotal, A.; Mandal, T. K.; Walt, D. R. *J. Polym. Sci., Part A: Polym. Chem.* **2005**, *43*, 3631−3642.

(15) Baum, M.; Brittain, J. W. *Macromolecules* **2002**, *35*, 610−615.

(16) Hu, T.; You, Y.; Pan, C.; Wu, C. *J. Phys. Chem. B* **2002**, *106*, 6659−6662.

(17) Hong, C. Y.; You, Y. Z.; Pan, C. Y. *J. Polym. Sci., Part A: Polym. Chem.* **2006**, *44*, 2419−2427.

(18) Bai, R. K.; You, Y. Z.; Pan, C. Y. *Polym. Int.* **2000**, *49*, 898−902.

(19) Huang, W.; Taylor, S.; Fu, K.; Lin, Y.; Zhang, D.; Hanks, T. W.; Rao, A. M.; Sun, Y.-P. *Nano Lett.* **2002**, *2*, 311−314.

(20) Mayadunne, R. T. A.; Rizzardo, E.; Chiefari, J.; Chong, Y. K.; Moad, G.; Thang, S. H. *Macromolecules* **1999**, *32*, 6977−6980.

(21) Li, Y. H.; Wang, S. G.; Luan, Z. K.; Ding, J.; Xu, C. L.; Wu, D. H. *Carbon* **2003**, *41*, 1057−1062.

(22) Ma, R. Z.; Sasaki, T.; Bando, Y. *J. Am. Chem. Soc.* **2004**, *126*, 10382−10388.

(23) Gao, C.; Vo, C. D.; Jin, Y. Z.; Li, W.; Armes, S. P. *Macromolecules* **2005**, *38*, 8634−8648.